ENGR241 Final Report

Team: Siddharth Doshi, Johan Carlström, and Bohan Li

Mentor: Stanley Lin, and Antonio Ricco

Stanford University, Stanford, California 94305

June 9th, 2023

Contents

1 Introduction

1.1 Motivation and Benefit to SNF community

PEDOT:PSS is a conductive polymer used in a great variety of scientific fields. It has been implemented in flexible and wearable electronics [1], solar cells [2], and nanophotonics [3]. At Stanford, PEDOT:PSS is also widely used by groups in bioelectronics, neural interfaces, chemical sensors, organic transistors, optical devices, etc. However, high-resolution structures are typically patterned using complex multi-step processes with unfavorable solvents. Here, we develop a novel, environmentally friendly direct electron beam writing technique of PEDOT:PSS, which can be widely used across Stanford. The process only requires a single step of electron beam lithography, with simple development in water, while maintaining PEDOT:PSS's favorable electrical, electrochemical, and electrochromic properties. Additionally, these structures are written at a resolution higher than achievable with normal lithography.

2 Process Development

2.1 Process Flow

The process flow for this single-step electron beam direct-write process is shown in figure 1a. First, the PEDOT:PSS is spin coated onto the substrate. Then, the electron beam lithography (EBL) process directly writes patterns onto PEDOT:PSS. The high energy electron beam alters PEDOT:PSS solubility in water, going from soluble to insoluble following electron beam exposure. Thus, PEDOT:PSS is functionally a negative electron beam lithography resist that can be developed in water. After exposure, the sample is developed in DI water for approximately 30 seconds until the unexposed PEDOT:PSS is dissolved.

This simple process eliminates multiple steps from the conventional process flow which requires EBL, evaporation of an etch mask, and subsequent etching (figure 1b). Removing the need of an etch mask leaves the PEDOT:PSS nanostructures free from unwanted residual materials on top. Such residual materials act as diffusion barriers for electrolytes and limit the performance of PEDOT:PSS-based switching devices.

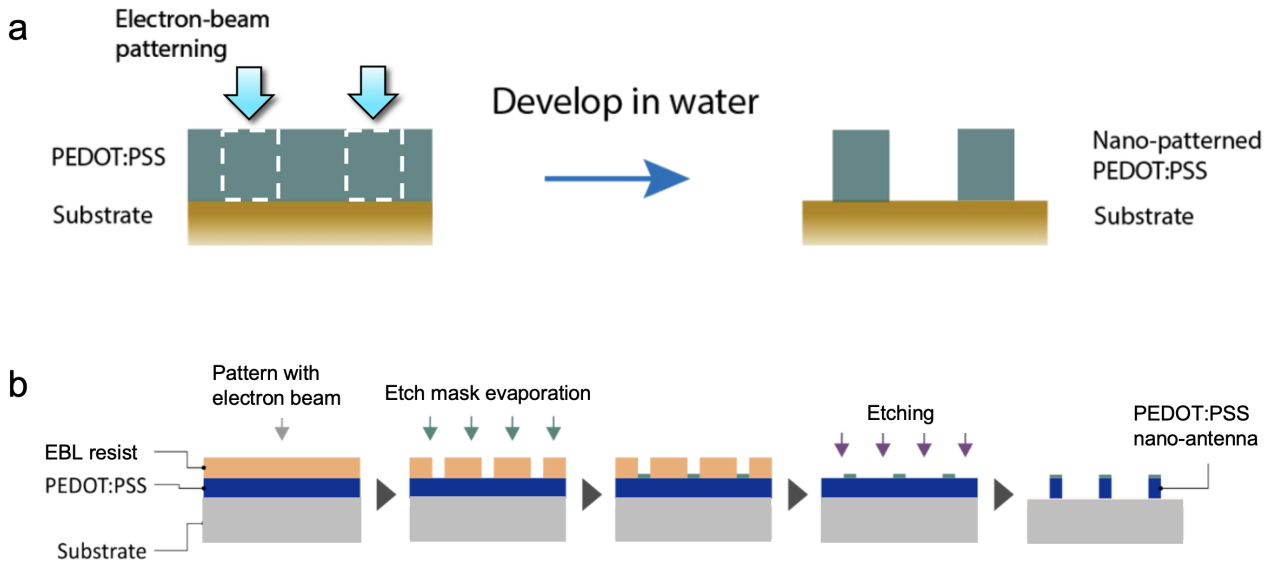

Figure 1: a) New developed single-step electron beam direct-write process flow for fabricating PEDOT:PSS nanostructures. b) Typical process flow for fabricating PEDOT:PSS nanostructures. In addition to being a complex multi-step process, it leaves a residual etch mask on top of the PEDOT:PSS structures.

2.2 Materials

All processes were developed using commercial PEDOT:PSS (Clevios PH1000, 1.3 wt percent) purchased from Ossila. To prepare a highly conductive PEDOT:PSS blend, ethylene glycol (5 wt percent) 1 drop of DBSA were added to PEDOT:PSS solution, followed by ultrasonication for 1 minute.

2.3 Spin Coating

Before spincoating, substrates are cleaned in Acetone and IPA, followed by 11 minutes of UV ozone cleaning using the Samco UV Ozone Cleaner UV-1 tool. The UV-ozone treatment make the substrate more hydrophilic which improves the PEDOT:PSS adhesion to the substrate.

The Headway Research Bowl Model CB15 spinner in the SNSF Nanopatterning Cleanroom is used for spin-coating. After spin-coating, the sample is heated on an 80°C hot plate for 10 seconds to evaporate any remaining liquid on the sample.

Film thicknesses between 70nm-120nm is achieved by varying the spin-speed. The relationship

between spin-speed vs thickness is summarized in table 1.

The process works for a range of substrates, including Au, ITO, Si and SiO_2. We note that due to variations in surface properties, each substrate will have a slightly different thickness vs spin-speed curve.

Spin Speed (RPM)	Film Thickness (nm)
1000	∼120nm
2000	∼90nm
3500	∼70nm

Table 1: PEDOT:PSS film thickness for a given spin-speed on Silicon.

2.4 Direct-write Electron Beam Lithography

To write nanostructures of PEDOT:PSS using electron beam lithography, we use the Raith Voyager with a 50kV acceleration voltage in the SNSF Nanopatterning Cleanroom. In order to establish a process window, we write dose matrices for a range of differently sized nanopillars. The electron beam step-size is kept constant at 5nm. We use a current of 320pA to ensure a small enough step size.

We first study the dose ranges required to write isolated nanostructures, then nanostructure arrays, before finally establishing parameters to write large-area PEDOT:PSS patterns, of relevance to applications in wearable and bioelectronics.

2.4.1 Patterning of Isolated Nanostructures

We find that smaller nanostructures require larger exposure doses in order to develop properly. This relationship is shown in figure 2b. The minimum feature size of isolated dots that is reliably achieved is 400nm, requiring 4000 $\mu C/cm^2$. For the dose range studied, we found that we could not properly develop smaller dots even at higher exposure doses of 5000 to 6000 μC/cm2. Figure 2a shows a scanning electron microscopy image of a subset of nanodot sizes after development.

Further details, including images of the dose response are found in the Appendix 7.

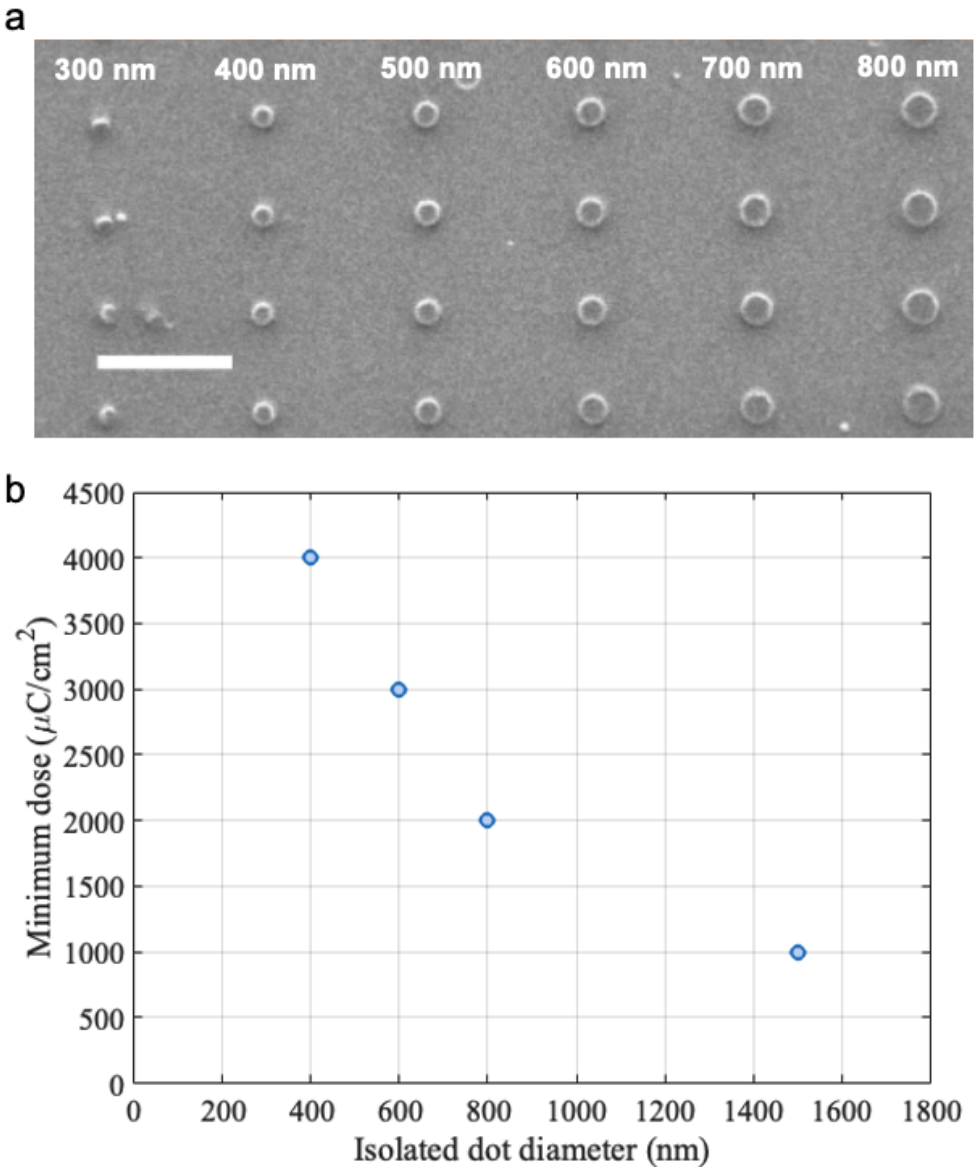

Figure 2: a) Scanning electron micoscopy image of isolated nano-dots. Below 400nm, no nano-dots survive development. Scale bar is 5 μm. b) Minimum exposure dose required to develop an isolated dot of a given diameter.

2.4.2 Patterning of Nanostructure Arrays

We look for a process window for writing dense arrays of PEDOT:PSS nanostructures. We define an acceptable dose range as between sufficiently high to leave a full-height pillar and sufficiently low to avoid exaggerated proximity effects in-between pillars. Figure 3a and b show optical micrographs of an "acceptable" array and "unacceptable" array, respectively.

Importantly, this process window depends on the filling fraction of the nanopillars. In general, higher filling fractions (smaller periods) result in a shrinking of the process window. The process window for each period for 90nm thickness PEDOT:PSS is summarized graphically in Figure 3c below.

Increasing the thickness also shrinks the process window, likely due to increased electron scattering through the thickness of the film and hence more significant proximity effects. We were not able to establish a process window for PEDOT:PSS nanostructures using a 120nm film thickness.

A detailed set of results, including nanostructure images are included in the Appendix 7.

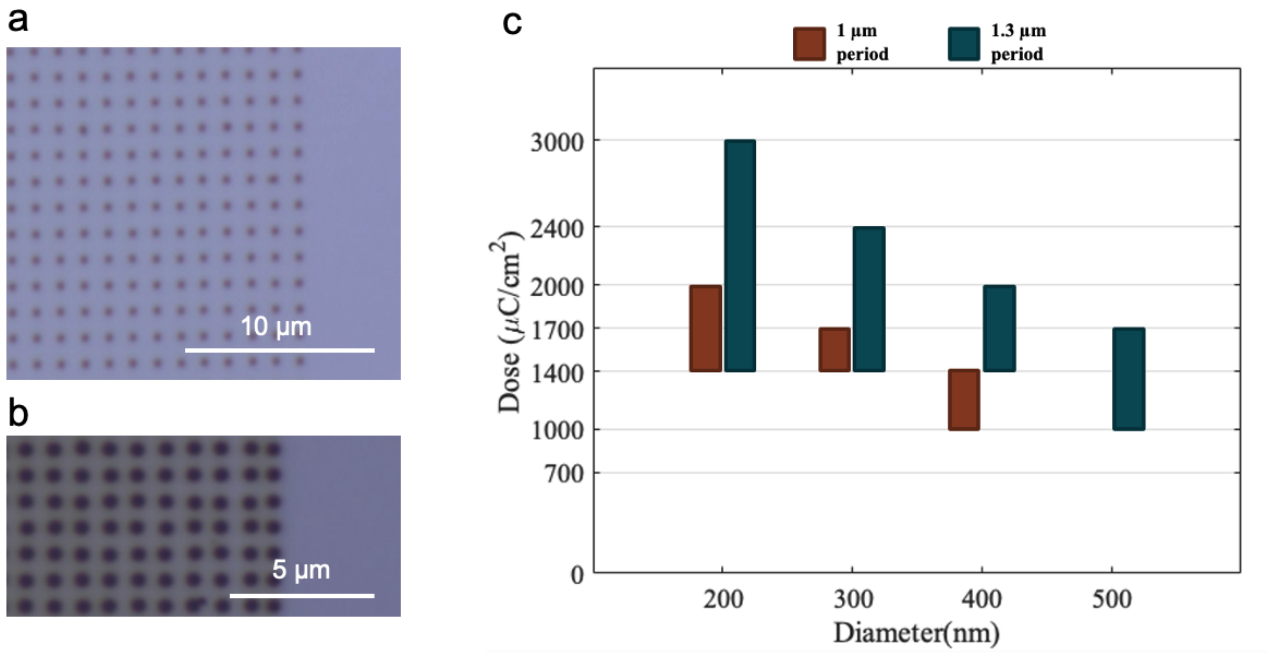

Figure 3: a) Optical micrograph of an array in the acceptable dose range with 400nm diameter and 1.3μm period. b) Optical micrograph of an array outside the acceptable range due to proximity effects with 500nm diameter and 1μm period. c) Graphical summary of the process window for two different periods. The shaded regions indicate process parameters deemed "acceptable".

2.4.3 Large Structure Patterning

To pattern macroscale (>1mm) structures, a dose-range of 250 - 500 μC/cm^2 is used. In order to write large structures within a reasonable time-frame, the beam current and step size is

set to 16nA and 15nm, respectively. These large area structures will be used in subsequent characterisation of electrical and electrochemical properties.

3 PEDOT:PSS Characterisation

Once a process window for the direct-write process is established, we want to make sure that PEDOT:PSS retains all its attractive properties after electron beam exposure. Therefore, thorough characterization of written PEDOT:PSS properties is necessary. In this section, we test the PEDOT:PSS properties before and after electron beam exposure. We characterise the electrical conductivity, electro-chemical properties, and optical switchability.

3.1 Electrical Conductivity

As a widely used conductive polymer, PEDOT:PSS has seen broad adoption into circuits and electronic devices. In these applications, the electrical conductivity is crucial. Therefore, we measure the electrical conductivity of PEDOT:PSS before and after electron beam exposure. Specifically, we use a four point probe measurement technique to measure sheet resistance to exclude the effect of contact resistance. To increase the reliability of the measurement results, we used two different four point probe measurement schemes: linear and van der Pauw.

3.1.1 Pristine PEDOT:PSS

First, we measure the sheet resistance of the pristine PEDOT:PSS without additional treatment using a four-point probe tool in Prof. Guosong Hong's lab. A schematic of the measurement is shown in Fig. 4a. To measure the sheet resistance of exposed PEDOT:PSS, we write large rectangles (6mm x 2mm) using electron beam lithography. The size was chosen for compatibility with the four point probe tool. Using the built-in calculation and empirical size corrections, the sheet resistance of the sample is extracted. For a better comparison between the unexposed and exposed PEDOT:PSS, we convert the sheet resistance to a conductivity (Fig. 4b).

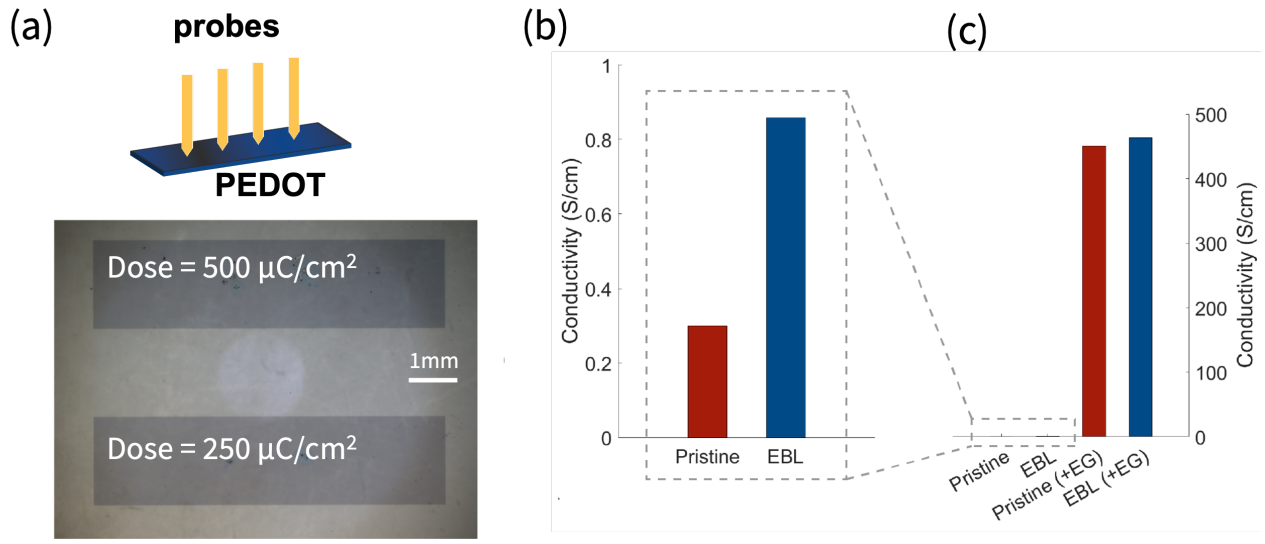

Figure 4: Conductivity measurement of pristine PEDOT:PSS after exposed to the electron beam. (a) The schematic diagram of the four-point probe measurement and the microscope image of the rectangular PEDOT sample. (b) The measured conductivity of pristine PEDOT:PSS before and after electron beam exposure, given as red and blue bars respectively. The displayed value is given by the mean of the conductivity measured at different electron beam doses. (c) The measured conductivity of the highly conductive PEDOT:PSS with additive chemicals (ethylene glycol) before and after electron beam exposure. The conductivity is at a similar level with and without electron exposure, which are both about three orders of magnitude greater than the pristine PEDOT:PSS.

The sheet resistance of the unexposed PEDOT:PSS is 1.3 Ω/square while it is 3.8 Ω/square for the exposed PEDOT:PSS. The conductivity is 30 S/m for unexposed case, which agrees with the value documented in the literature, and it is 85 S/m for the exposed case. The conductivity of the exposed sample is about three times greater than the unexposed sample, indicating the existence of some underlying processes alongside with electron beam exposure, which has an effect of enhancing electrical conductivity. We hypothesize that the electron beam exposure mainly interacts with the PSS part of the polymer, which breaks the chemical bonds of PSS and therefore changes its final composition between PEDOT and PSS after development. Since the conductivity of PEDOT:PSS comes from the PEDOT part and the PSS component mainly contributes to the resistivity, changing the relative composition can dramatically affect the electrical properties. Further characterization from the material perspective is needed to identify the full physical and chemical details.

In addition, comparing the cases with two different electron beam dose values, the conductivity

has minor variation, showing a rather stable conductivity value among the working dose range between 250 and 500 μC/cm^2. Therefore within the working range of valid electron beam exposure, the material property of PEDOT:PSS roughly stays the same.

To check the validity of the results, we re-measured the conductivity using the well-known van der Pauw scheme, With a similar working principle as the four-point probe measurement. The measured sheet resistance is given by 1.5×10^5 Ω/square, compared to 1.3×10^5 Ω/square measured using 4-point scheme. The result is of the same trend as the four-point measurement, with increasing conductivity after electron beam exposure and also without obvious structure geometry dependency.

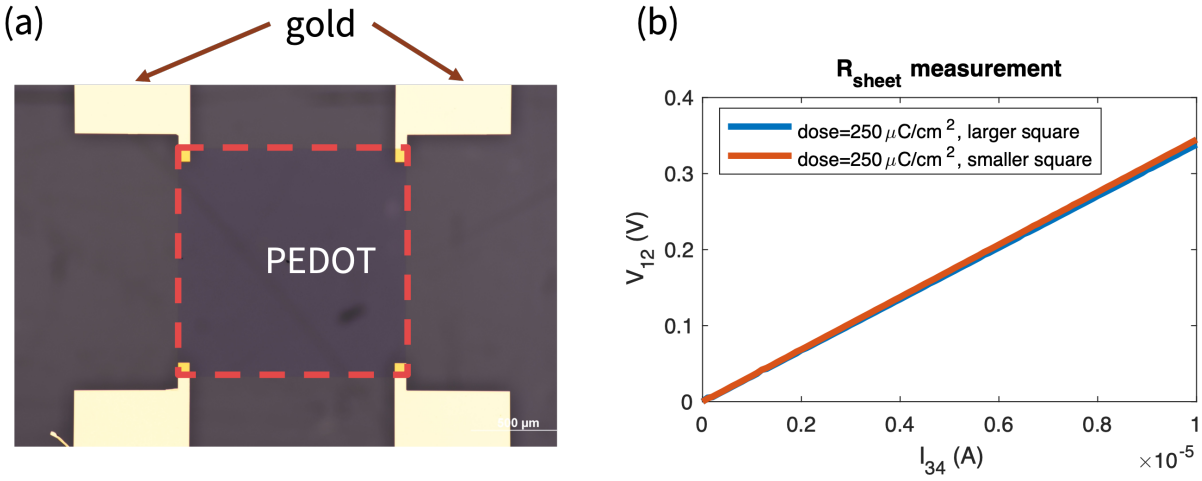

Figure 5: The sheet resistance measurement using the van der Pauw scheme. (a) The schematic diagram of the van der Pauw measurement with PEDOT:PSS patterned into a square and with gold contact attached at four corners. (b) The measured I-V curve of sheet resistance with electron beam dose at 250 $\mu C/cm^2$ and with two different square sizes.

3.1.2 High conductivity, additive enhanced PEDOT:PSS

For the broader research community of PEDOT electronics, it is usually not sufficient to use material of 40 S/m conductivity. To improve the electrical performance, in the literature, it is well-documented that the add-on chemicals can significantly enhance the PEDOT conductivity by roughly three orders of magnitude [4]. To test the influence of electron beam lithography on these highly-conductive PEDOT, we measured the sheet resistance again using the two schemes. The results are summarized in Fig. 4c, showing that exposure to the electron beam does not affect the conductivity. This indirectly supports the argument that electron beam exposure mainly reacts with the PSS component, degrading the PSS component which enhances

the conductivity. However, for the highly conductive PEDOT, the PSS is replaced by additives, therefore the electron beam exposure cannot induce a large change in the chemical composition, therefore the conductivity as well.

3.2 Electro-chromic Switching

PEDOT:PSS exhibits visible electrochromism. Upon application of electrochemical potential, ions are intercalated from the electrolyte solution into the material, resulting in modification of the oxidation state of the conjugated polymer backbone. This induces a change in optical properties, observed as a color change at visible wavelengths. We highlight the functionality of our structures by demonstrating color changes in an electron beam written Stanford logo as shown in Fig. 6.

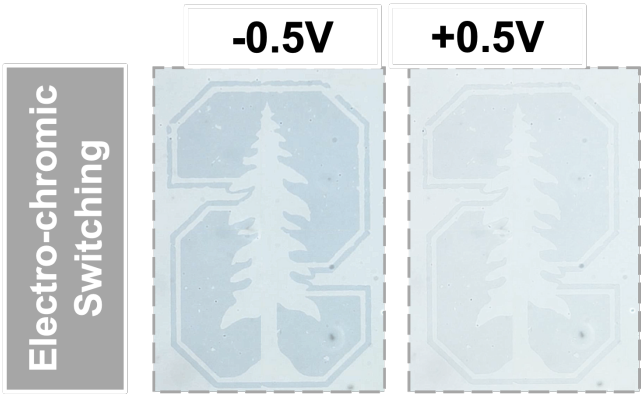

Figure 6: Demonstration of electro-chromic switching ability of PEDOT:PSS. The Stanford logo is directly patterned by exposing PEDOT:PSS with electron beam lithography. By changing the applied voltage from -0.5V to +0.5V, the color of the Stanford logo changes from light blue to light gray, and the definition of the features decreases.

We use a home-built electrochemical flow cell to allow for electrochemical switching of the polymer under a microscope objective with a three-electrode setup. Flow cells are constructed by sandwiching two pre-cut double-sided adhesive tapes between the sample and a glass coverslip. The sample area is larger than the coverslip area. An electrolyte pipetted onto the sample near the periphery of the coverslip is drawn into the flow cell by capillary action. The bottom gold sample serves directly as the working electrode (WE). The counter electrode (CE) (platinum wire) and the reference electrode (RE) (silver/silver-chloride pellet, Ag/AgCl pellet) are in contact with the exposed electrolyte (0.1 mol/l phosphate-buffered saline, or PBS) droplet that is at the periphery of the flow cell. A potentiostat (BioLogic SP-200) is used to control

the voltage that is applied relative to the reference. This system allows for electrochemical switching while maintaining optical access for reflectance microscopy.

As shown in Fig. 6, by switching the external voltage from +0.5V to -0.5V, the absorbance of the material increases at visible wavelengths increases. Application of negative voltage draws in positive ions from electrolyte solution to act as counter-ions for fixed negative charges in PSS, dedoping the PEDOT. The results in opening of a bandgap with energies matching optical frequencies, increasing the absorption and hence causing a change in colour.

3.3 Electro-chemical Characterisation

Samples were tested in a Teflon capture cell (Fig. 7) with an exposed area of 12cm^2. The electrolyte used was PBS (1x, 157mM salt concentration). Measurements were taken with a platinum wire counter electrode wrapped around an Ag/AgCl glass membrane reference electrode.

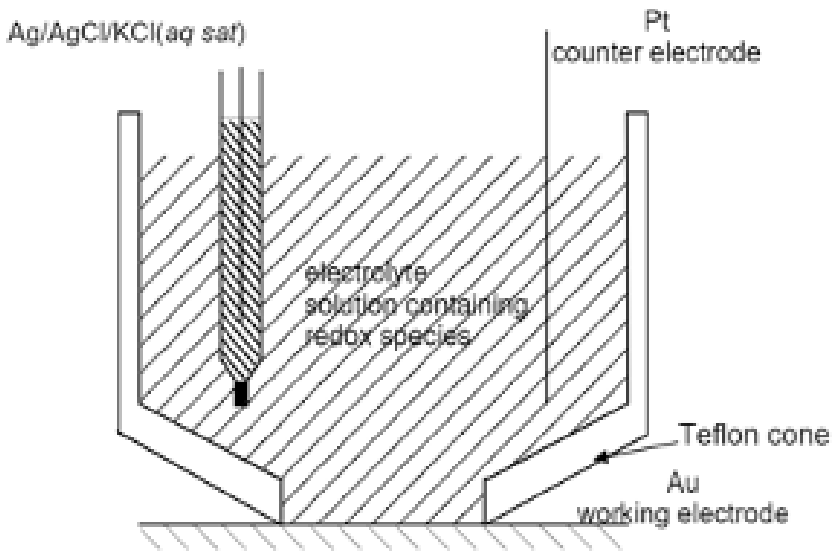

Figure 7: Schematic diagram of an electrochemical liquid cell used in the electro-chemical characterization.

Electrochemical Impedance Spectroscopy (EIS) was carried out from 1Hz to 1MHz with a 1mV variation around the open circuit voltage (OCV) of the material. Cyclic voltammetry was carried out by recording the measured current against applied voltage (vs. Ag/AgCl), cycled at a scan rate of 50mV/s. The results are shown in Fig. 8.

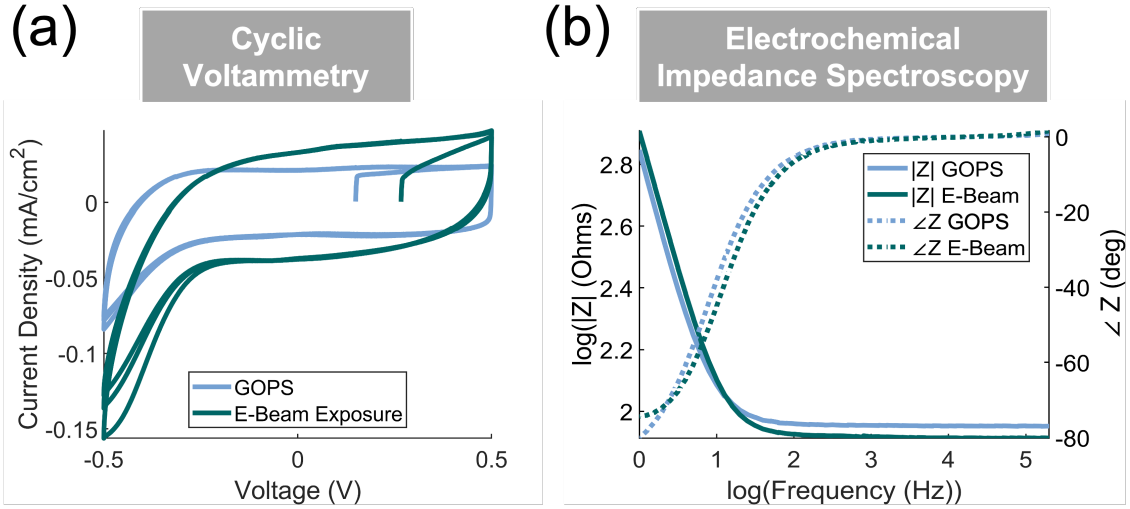

Figure 8: (a) The cyclic voltammetry measurement and the (b) impedance measurement of the conventionally cross-linked PEDOT:PSS using the "GOPS" method and of the electron beam lithography cross-linked PEDOT:PSS. The two schemes for cross-linking shows similar electro-chemical properties.

The cyclic voltammetry and electrochemical impedance spectroscopy results show that electron beam writing essentially preserves the electrochemical properties of PEDOT:PSS in aqueous electrolytes. This demonstrates it's relevance for biological applications, where traditionally, GOPS is used as a chemical crosslinker. The use of PEDOT:PSS could greatly simplify fabrication process for bioelectronic devices.

4 Conclusions

Throughout this project, we explore the possibility of a simple single-step direct-write process for writing PEDOT:PSS nanostructures. In particular, we study the working condition of electron beam lithography to achieve direct writing of various structures, including isolated nanodots, periodic arrays of nanodots, and larger patterns with millimeter sizes. In addition, for the broader research community, we test on the PEDOT:PSS properties before and after the electron beam exposure. The results show that the favorable properties all survive the electron beam exposure, which include the optical switchability, electrical properties, electrochemical properties. Therefore, this direct-write process paves the way of writing PEDOT:PSS nanostructures while preserving the special material properties, which in the future can be implemented to speed up the process flow of relevant research area, inlcuding PEDOT:PSS

nanophotonics, flexible electronics, and so on.

5 Acknowledgement

We sincerely appreciate the support from the Stanford Nanofabrication Facilities (SNF) and the Stanford Nano Shared Facilities (SNSF). Special thanks to our mentors Stanley Lin and Antonio Ricco for guidance and support. Thanks to all the collaborators, Dominik Ludescher, Julian Karst, Moritz Flöß, Mario Hentschel, Nofar Hemed, and Harald Giessen for useful discussions. Thanks to the Hong lab for their support on the sheet resistance measurements. Thanks to Christina Newcomb for the suggestions and guidance on atomic force microscope measurements. Thanks to all the members of ENGR241 for enlightening suggestions.

6 Budget

The total budget of this project is $4982.55, which can be divided into $3744.55 tool usage cost (major part: electron beam lithography and atomic force microscope), $925 tool training cost, and $310 for supply purchases.

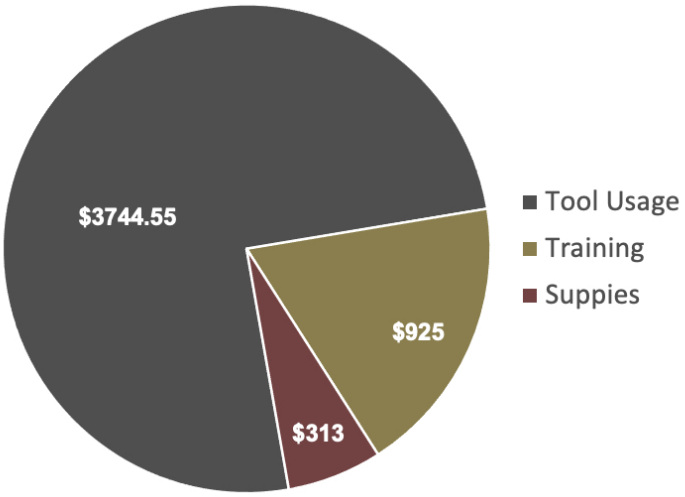

Figure 9: Funding usage during the class.

7 Appendix

7.1 Dose Matrix of Isolated Nanodots

A dose matrix test is done to acquire the dose range for writing isolated nanodots. The micrographs are shown in Fig. 10 with electron beam dose varying from 1000 $\mu C/cm^2$ on the top panel to 5000 $\mu C/cm^2$ on the bottom panel. The size of the nanodots increases from 100 nm on the leftmost column to 1500 nm on the rightmost column with 100 nm increment between each column. The minimum dot size is 400 nm written with 4000 $\mu C/cm^2$. For even smaller sizes, the feature is completely washed away during the development procedure. Comparing nanodots written at different dose values, the nanodots of a smaller size are underdefined with shifted position or distorted shape, similar to the case comparing the dots of different sizes but written at the same dose value. Therefore from this dose matrix test, it can be concluded that a higher amount of electron beam dose is required to write isolated nanodots of smaller size.

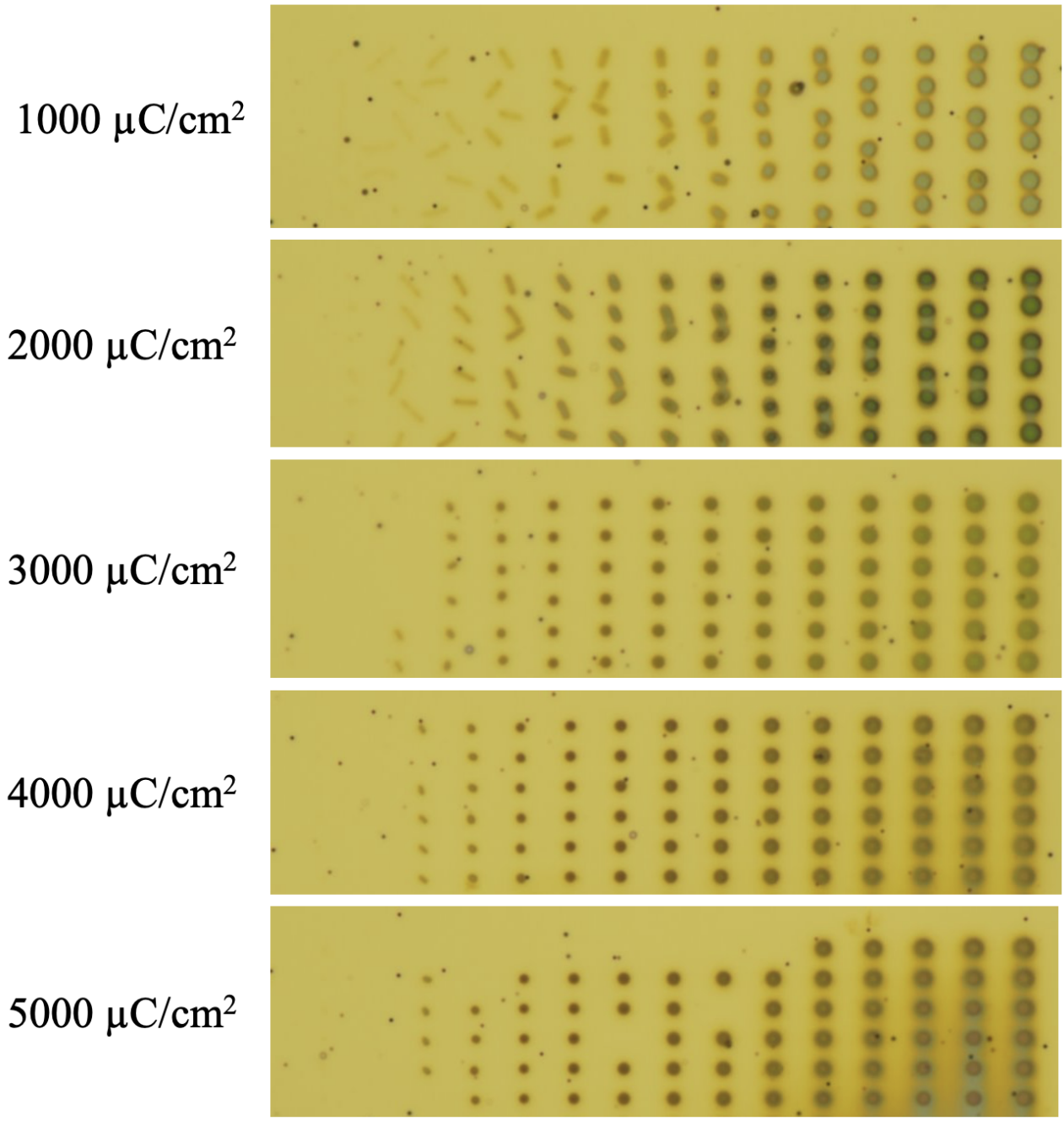

Figure 10: Dose-matrices of nanodots of varying sizes. The largest dots is 1.5 μm and they are incrementally smaller (100nm steps) going from right to left.

7.2 Dose Matrix of Periodic Array of Nanodots

A dose matrix test is done to acquire the acceptable dose range for writing periodic arrays of nanodots, where the results are shown in Fig. 11.

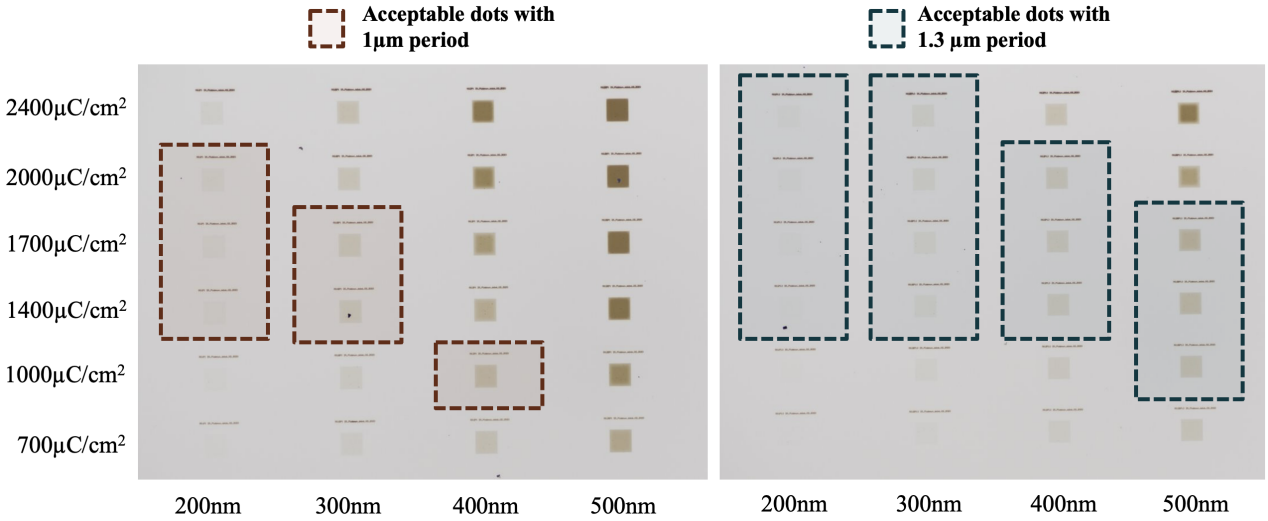

Figure 11: Dose-test for nanodot arrays with varying dot size. The left and right panel has a constant period of $1\mu m$ and 1.3 μm, respectively. Boxed areas indicated region with "acceptable" dose conditions.

References

[1] Hyunwoo Yuk, Baoyang Lu, Shen Lin, Kai Qu, Jingkun Xu, Jianhong Luo, and Xuanhe Zhao. 3d printing of conducting polymers. *Nature communications*, 11(1):1604, 2020.

[2] Jian He, Pingqi Gao, Zhaoheng Ling, Li Ding, Zhenhai Yang, Jichun Ye, and Yi Cui. High-efficiency silicon/organic heterojunction solar cells with improved junction quality and interface passivation. *ACS nano*, 10(12):11525–11531, 2016.

[3] Julian Karst, Moritz Floess, Monika Ubl, Carsten Dingler, Claudia Malacrida, Tobias Steinle, Sabine Ludwigs, Mario Hentschel, and Harald Giessen. Electrically switchable metallic polymer nanoantennas. *Science*, 374(6567):612–616, 2021.

[4] Dion Khodagholy, Thomas Doublet, Moshe Gurfinkel, Pascale Quilichini, Esma Ismailova, Pierre Leleux, Thierry Herve, Sébastien Sanaur, Christophe Bernard, and George G Malliaras. Highly conformable conducting polymer electrodes for in vivo recordings. *Advanced Materials*, 23(36):H268–H272, 2011.